Practical output regulation and tracking for linear ODE-hyperbolic PDE-ODE systems

Jeanne Redaud, Federico Bribiesca-Argomedo, Jean Auriol

Chapter 1
Practical output regulation and tracking for linear ODE-hyperbolic PDE-ODE systems

Jeanne Redaud, Federico Bribiesca-Argomedo, Jean Auriol

Abstract In this chapter, we consider the problem of practical output regulation and output tracking for a linear 2×2 hyperbolic Partial Differential Equation (PDE) system with actuation and load dynamics. Indeed, it is actuated via an Ordinary Differential Equation (ODE) at one boundary and the output to be controlled is the output of an ODE at the other boundary. The main focus is on load tracking. Here, we propose to extend existing results on approximate output regulation to a class of systems similar to that considered in [8] and to extend filtering techniques to a dynamically augmented system with finite-dimensional exosystems considering possible trajectory and disturbance inputs. Issues with respect to small delays in the state reconstruction and feedback loop are considered. Due to the nature of the disturbances, the state estimation and disturbance reconstruction problems are also considered. This scenario finds applications in many systems of engineering interest, such as drilling systems [3], pneumatic systems [17], or electric transmission lines [22].

Jeanne Redaud
Université Paris-Saclay, CNRS, CentraleSupélec, Inria Saclay, Laboratoire des Signaux et Systèmes, 91190, Gif-sur-Yvette, France, e-mail: jeanne.redaud@centralesupelec.fr

Federico Bribiesca-Argomedo
Université de Lyon, INSA Lyon, Laboratoire Ampère (CNRS UMR5005) - F-69621 Villeurbanne, France, e-mail: federico.bibriesca-argomedo@insa-lyon.fr

Jean Auriol
Université Paris-Saclay, CNRS, CentraleSupélec, Inria Saclay, Laboratoire des Signaux et Systèmes, 91190, Gif-sur-Yvette, France, e-mail: jean.auriol@centralesupelec.fr

1.1 Introduction

In this chapter, we consider a linear 2×2 hyperbolic Partial Differential Equation (PDE) coupled at one end with an actuator and on the other end with a load, both modeled by potentially unstable Ordinary Differential Equations (ODE). The main focus is on load tracking (i.e. tracking an output depending on the states of the unactuated ODE, while only controlling the opposite ODE system) and disturbance rejection. More precisely, we design a dynamic full-state feedback control law acting only on the first ODE system (the actuator) and ensuring that an output, depending on the states of the opposite ODE system (the unactuated load), follows a prescribed trajectory generated by a finite-dimensional exosystem. This tracking property holds in the presence of exogenous disturbances (modeled by a known finite-dimensional system) acting on the load.

Since transport phenomena and delays are common in industrial applications, many systems can be modeled by hyperbolic PDEs, such as oil drilling pipes [2, 25], pneumatic systems [17], networks of hydraulic distribution lines or electrical lines [6, 22]. Such systems can be coupled with ODE dynamics that represent loads or actuator dynamics. In different applications, the distal ODE state can model the dynamics of a suspended object or payload for Unmanned Aerial Vehicles (UAV) [15] or the Bottom Hole Assembly at the end of a drilling pipe [5], to cite some examples. More specifically, the ODE-PDE-ODE structure naturally arises when considering linear systems of balance laws with finite-dimensional actuator and load dynamics, as for the UAV-cable-payload structure [25].

Therefore, coupled hyperbolic PDEs and ODEs have been an active research field in the previous years. The stabilization of each independent subsystem is a well-known task. Indeed, PID or Smith Predictor controllers have been extensively developed for linear ODEs [23]. Moreover, the well-known backstepping technique has been adapted to provide constructive designs of control laws for hyperbolic systems [18]. Finally, output regulation problems have already been solved for hyperbolic systems without actuator and load dynamics [1].

However, new problems have to be overcome when ODEs and PDEs are interconnected. The backstepping method has then been adapted to such systems. First, only PDE-ODE interconnections were considered [12]. Next, some results have been extended to ODE-PDE-ODE interconnections, and full-state feedback controllers have been designed for such coupled systems. In most cases, the constructive design is based on several invertible backstepping transforms. They are used to cancel the reflection term on the actuated boundary such that the PDE has no longer an impact onto the state of the controlled ODE [7, 10].

However, suppression of the reflection term may lead to non strictly proper control laws. This can cause robustness issues, leading in particular to unstable behaviors in the presence of arbitrary small delays [4]. This is, therefore, a

significant concern for further application to real systems. Consequently, the focus has been made on robustly stabilizing such systems. Instead of canceling all the reflection terms at the actuated boundary, [13] assigned it the dynamics of a low-pass filter. In [8], the authors proposed a strictly proper control law guaranteeing a non-zero delay margin in closed-loop and stabilizing the coupled ODE-PDE-ODE structure, using filtering techniques. However, the stabilizing control law from [8] requires the knowledge of all the states. In this chapter, we extend the proposed approach to an output feedback control law and design an observer for the coupled system. This result is closely related to that in [25]. However, the specific observer design proposed here does not require multiple transforms. Unlike [25], all the error injection terms used in the proposed observer are strictly proper, which avoids having arbitrarily big gains at high frequencies (typically amplifying measurement noise).

Furthermore, instead of focusing on stabilizing the interconnected system (bringing it back to an equilibrium state), we solve the problem of practical output regulation and output tracking. Indeed, the ODE system opposite to the control input can be subject to perturbation. We extend the results in [8] to a dynamically augmented system with a finite-dimensional exosystem corresponding to a possible trajectory reference or/and to a disturbance input. The problem of disturbance reconstruction and the state estimation are also addressed in the proposed observer.

More specifically, the contribution of this chapter is to propose a constructive approach for the design of a dynamic, strictly proper, output-feedback control law for practical output regulation and output tracking, guaranteeing a non-zero delay margin for a large class of interconnected ODE-hyperbolic PDEs-ODE systems. This approach can be easily implemented on real systems. Unlike [25, 10], it does not require to apply multiple successive state transformations, which simplifies the design and implementation procedure for field engineers who are not familiar with multi-step approaches. Moreover, it is based on assumptions that can be easily tested in practice.

The proposed approach can be summarized as follows. Based on some structural assumptions, and inspired by the approach proposed in [8], we first design a state-feedback controller to stabilize an output depending on the states of the unactuated ODE, solving thereby the practical output tracking and regulation problem. We follow the backstepping methodology and use a general invertible integral transform to map our initial system (dynamically augmented with finite-dimensional exosystems) to a target system. We use a frequency analysis to design a feedback controller. Using structural assumptions similar to those in [25], we then propose a state observer design for the system and the disturbances. Unlike [25], we use filtering techniques to guarantee that all the dynamic error injection gains are strictly proper. Finally, the two designs are coupled in order to obtain a dynamic output feedback controller.

The layout of this chapter is the following: in Section 1.2, we present the structure of the system and give some structural assumptions. Next, we design

a robust state feedback controller for practical output regulation in Section 1.3. We design an observer for the state and the perturbation in Section 1.4. Finally, we propose some illustrative examples with test-cases simulations in Section 1.5.

Notation
In the following, we denote $\mathcal{T}^+$ the upper-triangular domain defined in $\mathbb{R}^2$ by $\mathcal{T}^+ \doteq \{(x,y) \in [0,1]\times[0,1], y \geq x\}$, and $\mathcal{T}^-$ the lower-triangular domain defined by $\mathcal{T}^- \doteq \{(x,y) \in [0,1]\times[0,1], y \leq x\}$. Given a set $[a,b] \in \mathbb{R}$, we define the characteristic function $\mathbb{1}_{[a,b]}(x) \doteq 1$, if $x \in [a,b]$, 0 otherwise. The euclidean norm of a vector $\varphi \in \mathbb{R}^r$, $r \in \mathbb{N}\backslash\{0\}$ is denoted by $\|\varphi\|_{\mathbb{R}^r} \doteq (\varphi^\intercal\varphi)^{1/2}$. The L_2-norm of a function $\phi \in L^2([0,1];\mathbb{R})$ is taken in the usual sense $\|\phi\|_{L^2} = \left(\int_0^1 \phi^2(s)\mathrm{d}s\right)^{1/2}$. We denote $\mathcal{X} \doteq \mathbb{R}^n \times L^2([0,1];\mathbb{R})^2 \times \mathbb{R}^{m+p}$ the space of the states of the system $(X(t), u(t,\cdot), v(t,\cdot), Y(t))$. We define the $\mathcal{X}-$norm of the state (X,u,v,Y) as the sum of these norms: $\|(X,u,v,Y)\|_{\mathcal{X}} \doteq \|X\|_{\mathbb{R}^n} + \|Y\|_{\mathbb{R}^{m+p}} + \|u\|_{L^2} + \|v\|_{L^2}$.
The notation I_r represents the $r \times r$ identity matrix. For any matrix A, we denote its transpose A^T and its conjugate transpose (or Hermitian transpose) A^*. We use $\mathscr{L}(\phi)(s)$ to denote the Laplace transform of $\phi(t)$. For any proper and stable transfer matrix $G(s)$, $\bar{\sigma}(G(j\omega))$ stands for the largest singular value of $G(j\omega)$ at frequency ω, and the H_∞-norm of G is $\|G\|_\infty = \operatorname{ess\,sup}_{\omega\in\mathbb{R}} \bar{\sigma}(G(j\omega))$.

1.2 Problem Statement

In this section, we present the system considered herein in more details, and we outline the control strategy. We also give some structural assumptions used in the following sections.

1.2.1 System presentation

Let us consider a linear 2×2 hetero-directional hyperbolic PDE system interconnected at both ends with an ODE system. The first ODE system $(X(t) \in \mathbb{R}^{n\times 1})$, is actuated by a control input $U(t) \in \mathbb{R}^{c\times 1}$, and the second ODE system $(Y_1(t) \in \mathbb{R}^{m\times 1})$ is dynamically augmented by an exosystem $(Y_2(t) \in \mathbb{R}^{p\times 1})$, such that $Y(t) = \begin{bmatrix} Y_1(t) \\ Y_2(t) \end{bmatrix} \in \mathbb{R}^{(m+p)\times 1}$. The exogenous input encompasses a disturbance Y_{pert} and/or a known reference trajectory Y_{ref}, as illustrated in Section 1.5. Following the notations given in Figure 1.1, we can model the system dynamics by the following set of equations

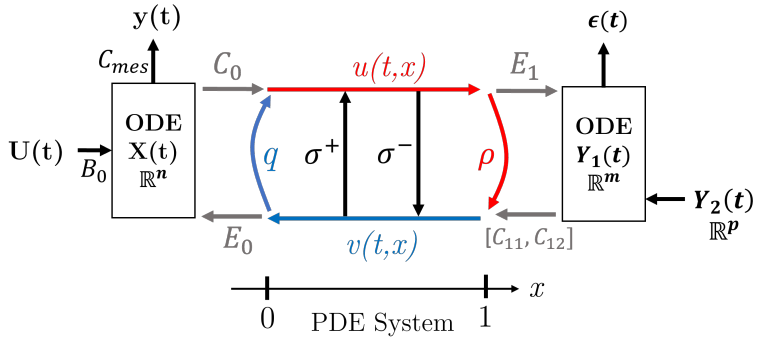

Fig. 1.1 Schematic presentation of the system

$$\dot{X}(t) = A_0 X(t) + E_0 v(t,0) + B_0 U(t), \tag{1.1}$$
$$u_t(t,x) + \lambda u_x(t,x) = \sigma^+(x) v(t,x), \tag{1.2}$$
$$v_t(t,x) - \mu v_x(t,x) = \sigma^-(x) u(t,x), \tag{1.3}$$
$$\dot{Y}(t) = \begin{bmatrix} A_{11} & A_{12} \\ 0_{p\times m} & A_{22} \end{bmatrix} Y(t) + \begin{bmatrix} E_1 \\ 0_{p\times 1} \end{bmatrix} u(t,1), \tag{1.4}$$

with $(t,x) \in [0,+\infty) \times [0,1]$, and the boundary conditions

$$v(t,1) = \rho u(t,1) + \begin{bmatrix} C_{11} & C_{12} \end{bmatrix} Y(t), \tag{1.5}$$
$$u(t,0) = q v(t,0) + C_0 X(t), \tag{1.6}$$

with non scalar ODE dynamics of dimension $n, m, p, c \in \mathbb{N}\backslash\{0\}$, and $A_0 \in \mathbb{R}^{n\times n}$, $E_0 \in \mathbb{R}^{n\times 1}$, $B_0 \in \mathbb{R}^{n\times c}$, $A_{11} \in \mathbb{R}^{m\times m}$, $A_{12} \in \mathbb{R}^{m\times p}$, $A_{22} \in \mathbb{R}^{p\times p}$, $E_1 \in \mathbb{R}^{m\times 1}$, $C_0 \in \mathbb{R}^{1\times n}$, $C_{11} \in \mathbb{R}^{1\times m}$ and $C_{12} \in \mathbb{R}^{1\times p}$. We suppose that the transport velocities $\lambda, \mu > 0$ are constant for sake of simplicity. Similarly, the boundary couplings $q, \rho \in \mathbb{R}$ are assumed constant, but the in-domain couplings between the PDEs $\sigma^+, \sigma^- \in C([0,1];\mathbb{R})$ are space-dependent functions. Let us consider any initial conditions $(X_0, u_0, v_0, Y_0) \in \mathcal{X}$. The system (1.1)-(1.6) is well-posed in a weak sense [6, Appendix A], i.e. it admits a solution in $\mathcal{X}$. We assume that we measure a part of the first ODE state, such that $y(t) = C_{\text{mes}} X(t) \in \mathbb{R}^{n'\times 1}$. The structure presented herein is motivated by drilling applications. Indeed, the ODEs can model the non negligeable dynamics of the top-drive at the surface, and the Bottom Hole Assembly (BHA) at the end of the pipe. The hyperbolic PDEs can represent torsional or axial wave-like propagation. Measurement and actuation are then only available at the surface ($x = 0$). However, due to the symmetry of the problem, we could have considered measurement in $x = 1$. In this paper, we assume that the rock interaction has an impact on the BHA and the boundary of the PDE, such that the

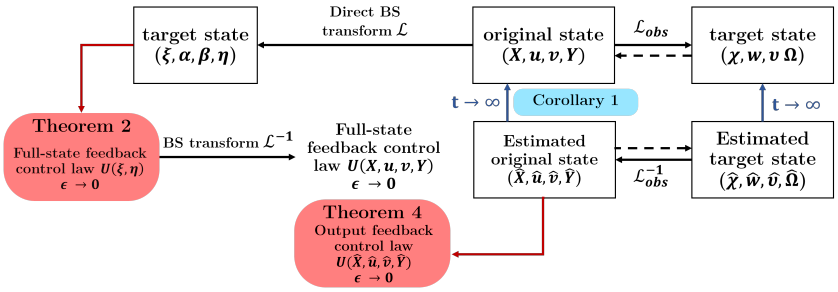

Fig. 1.2 Schematic presentation of the output-feedback control design

friction along the pipe is neglected. It allows a simpler regulation design, but distributed disturbance was considered for output regulation in [11].

1.2.2 Control strategy

The objective of this chapter is to design a control law $U(t)$ guaranteeing the approximate regulation to zero of a virtual output $\epsilon(t)$ defined by

$$\epsilon(t) \doteq C_e Y(t), \quad \text{with } C_e = \begin{bmatrix} C_{e1} & C_{e2} \end{bmatrix}. \tag{1.7}$$

In most cases, $\epsilon(t) \in \mathbb{R}$ is a scalar function ($C_{e1} \in \mathbb{R}^{1\times m}, C_{e2} \in \mathbb{R}^{1\times p}$). Therefore, we can only stabilize a linear combination of components of the extended state.
The stabilization of ϵ fulfills the trajectory tracking and perturbation rejection objectives, depending on the value of C_e. Generally speaking, we want the unactuated ODE state to robustly converge towards a known reference trajectory even in the presence of a disturbance.
The design of a robust output-feedback controller is schematically represented on Figure 1.2. First we follow the backstepping methodology to map our initial system to a simpler target system, using an invertible integral transform. Then, we use frequency analysis to show that this constructive approach leads to a control law solving the practical output regulation/output tracking problem. Inspired by [8], we apply filtering techniques to guarantee the delay-robustness of the proposed controller. Next, we solve the problem of state estimation and disturbance reconstruction.

1.2.3 Structural assumptions

Throughout this chapter, we use several assumptions on the system.

Assumption 1 The coefficients ρ, q satisfy $|\rho q| < 1$ and $\rho q \neq 0$. □

This assumption is sufficient and can be easily tested, compared to numerical computation of eigenvalues. The fact that $|\rho q| < 1$ is nearly necessary to guarantee a delay-robustness margin [4] (in the case $|\rho q| = 1$, it could be robust under specific conditions). Else, we could have an infinite number of poles in the closed right-half plane, in which case any (potentially dynamic) linear control law would lead to a zero delay margin [20], meaning that it could not be implementable and relevant for industrial applications.

Assumption 2
The pairs (A_0, B_0) and (A_{11}, E_1) are stabilizable (i.e. there exist $F_0 \in \mathbb{R}^{p\times n}$, $F_1 \in \mathbb{R}^{1\times m}$ such that $\bar{A}_0 \doteq A_0 + B_0F_0$ and $\bar{A}_{11} \doteq A_{11} + E_1F_1$ are Hurwitz). □

The two conditions in Assumption 2 are quite natural and can be easily numerically tested when implemented. The stabilizability of (A_{11}, E_1) is necessary and implies that the second ODE system can be stabilized in absence of perturbation independently of the PDE or interconnection structure. The condition on (A_0, B_0) allows for a simpler design of the control law, as it will appear in Section 1.3.1.

Assumption 3
The matrices $(\bar{A}_0, B_0, C_0)$ satisfy

$$\operatorname{rank}\left(\begin{bmatrix} sI - \bar{A}_0 & B_0 \\ C_0 & 0_{1\times c} \end{bmatrix}\right) = n + 1, \quad \forall s \in \mathbb{C}, \mathrm{Re}(s) \geq 0.$$

As before, this assumption allows a simpler controller design, and serves several purposes. First, it implies that C_0 is not identically zero, and in particular, admits a right inverse since it is necessarily full row rank. Indeed, if it was not the case, it would have obstructed the stabilization of the PDE and Y_1 subsystems through X in the absence of perturbation. Then, it is also equivalent (under Assumption 2) with the transfer matrix $P_0(s) \doteq C_0(sI - \bar{A}_0)^{-1}B_0$ having no zeros in the complex right-half plane that are common to all its components. Consequently, $P_0(s)$ admits a stable right-inverse (which, in general, is not proper). We denote $P_0^+(s)$ any such right inverse.

Assumption 4
The matrix A_{22} is marginally stable. Also, there exist matrices $T_a \in \mathbb{R}^{m\times p}, F_a \in \mathbb{R}^{1\times p}$ solutions to the *regulator equations*:

$$\begin{cases} -A_{11}T_a + T_aA_{22} + A_{12} = -E_1F_a, \\ -C_{e1}T_a + C_{e2} = 0. \end{cases} \tag{1.8}$$

This assumption gives a sufficient structural condition for the existence of a solution for the output regulation problem [14]. This is a condition on the invariant zeros of the plant and the spectrum of the exosystem. More precisely, A_{11} and A_{22} have disjoint spectra, and the number of outputs we regulate (one in the case ϵ scalar) is coherent with the number of inputs (c). The matrices T_a, F_a can be computed using a Schur triangulation.

Since observation is a dual problem to stabilization, sufficient assumptions corresponding to Assumptions 2, 3 are formulated for the observer design.

Assumption 5

The pairs (A_0, C_{mes}) and $(\begin{bmatrix} A_{11} & A_{12} \\ 0_{p\times m} & A_{22} \end{bmatrix}, \begin{bmatrix} C_{11} & C_{12} \end{bmatrix})$ are detectable (i.e. there exist $L_X \in \mathbb{R}^{p\times n'}$, $L_1 \in \mathbb{R}^{m\times 1}$, $L_2 \in \mathbb{R}^{p\times 1}$ such that $A_0^{\text{obs}} \doteq A_0 + L_X C_{\text{mes}}$ and $A_1^{\text{obs}} \doteq \begin{bmatrix} A_{11} & A_{12} \\ 0_{p\times m} & A_{22} \end{bmatrix} + \begin{bmatrix} L_1 \\ L_2 \end{bmatrix} \begin{bmatrix} C_{11} & C_{12} \end{bmatrix}$ are Hurwitz). □

Assumption 6

The matrices $(A_0^{\text{obs}}, E_0, C_{\text{mes}})$ satisfy

$$\text{rank}\left(\begin{bmatrix} sI - A_0^{\text{obs}} & E_0 \\ C_{\text{mes}} & 0_{n'\times 1} \end{bmatrix}\right) = n + 1, \quad \forall s \in \mathbb{C}, \text{Re}(s) \geq 0.$$

This assumption implies that the column vector E_0 is not identically zero, and in particular admits a left inverse. Moreover, it implies that the transfer matrix $P_{\text{mes}}(s) \doteq C_{\text{mes}}(sI - \bar{A}_0)^{-1}E_0$ has no zeros in the complex right-half plane and admits a stable left-inverse (which is not proper).
Note that all assumptions can be easily tested before implementation, in order to simplify the use of this methodology for field engineers.

1.3 State-feedback controller design

In this section, we extend the results from [8] to a dynamically augmented system with a finite-dimensional exosystem whose state is denoted $Y_2(t)$. First, we follow the backstepping methodology to map our initial system to a simpler target system. We show that the integral transform we use is invertible. Next, a frequency analysis of the target system is made. Filtering techniques are used to guarantee the robustness of the full-state feedback control law, designed to solve the initial practical output tracking/output regulation problem. Our objective is to stabilize the virtual output $\epsilon(t)$, which is a combination of the unactuated ODE state $Y_1(t)$ and the exogenous state $Y_2(t)$.

1.3.1 Backstepping transform

In order to map the initial system (1.1)-(1.6) onto a simpler target system, we use the following integral transform

$$X(t) = \xi(t) + \int_0^1 M^{12}(y)\alpha(t,y) + M^{13}(y)\beta(t,y)\mathrm{d}y + \left[M^{14}\ M^{15}\right]\eta(t), \tag{1.9}$$

$$\begin{aligned} u(t,x) &= \alpha(t,x) + \int_x^1 M^{22}(x,y)\alpha(y) + M^{23}(x,y)\beta(y)\mathrm{d}y + \left[M^{24}(x)\ M^{25}(x)\right]\eta(t), \\ v(t,x) &= \beta(t,x) + \int_x^1 M^{32}(x,y)\alpha(y) + M^{33}(x,y)\beta(y)\mathrm{d}y + \left[M^{34}(x)\ M^{35}(x)\right]\eta(t), \\ Y(t) &= \eta(t), \end{aligned} \tag{1.10}$$

with kernel gains and kernel functions $M^{12}, M^{13} \in C([0,1];\mathbb{R}^{n\times 1})$, $M^{14} \in \mathbb{R}^{n\times m}$, $M^{24}, M^{34} \in C([0,1];\mathbb{R}^{1\times m})$ (resp. $M^{15} \in \mathbb{R}^{n\times p}$, $M^{25}, M^{35} \in C([0,1];\mathbb{R}^{1\times p})$), and $M^{22}, M^{23}, M^{32}, M^{33} \in C(\mathcal{T}^+;\mathbb{R})$. Note that this change of variables is well-defined, since the transform is composed of identity functions, integral operators with regular kernels and matrices, and is therefore bounded. Due to its inner upper triangular structure, with identities and invertible Volterra integral operators on the diagonal, it is invertible [24, 26]. The inverse transform $\mathcal{L}$ (using a direct formulation) has the same structure, with coefficients K^{ij} expressed in terms of M^{ij} (and reciprocally) [19].

1.3.2 Target system

Let us consider the target state $(\xi,\alpha,\beta,\eta) \in \mathcal{X}$, where $\eta(t) = \begin{bmatrix}\eta_1(t)\\ \eta_2(t)\end{bmatrix}$ is decomposed into two parts. These new variables satisfy the following set of equations

$$\begin{aligned} \dot{\xi}(t) &= \bar{A}_0\xi(t) - \lambda M^{12}(0)C_0\xi(t) + \bar{E}_1\alpha(t,1) + \bar{E}_0\beta(t,0) \\ &\quad + \left[M_1\ M_p\right]\eta(t) + \int_0^1 M^{\alpha}(y)\alpha(t,y) + M^{\beta}(y)\beta(t,y)\mathrm{d}y + B_0\tilde{U}(t), \end{aligned} \tag{1.11}$$

$$\alpha_t(t,x) + \lambda\alpha_x(t,x) = 0, \quad \beta_t(t,x) - \mu\beta_x(t,x) = 0, \tag{1.12}$$

$$\dot{\eta}(t) = \begin{bmatrix}\bar{A}_{11} & \bar{A}_{12}\\ 0 & A_{22}\end{bmatrix}\eta(t) + \begin{bmatrix}E_1\\ 0_{p\times 1}\end{bmatrix}\alpha(t,1), \tag{1.13}$$

with the boundary conditions

$$\alpha(t,0) = q\beta(t,0) + C_0\xi(t), \quad \beta(t,1) = \rho\alpha(t,1), \tag{1.14}$$

with $\bar{A}_0, \bar{A}_{11}$ are defined by Assumption 2, and the other coefficients by

$$\bar{A}_{12} = A_{12} + E_1(F_a + F_1 T_a), \quad \bar{E}_0 = E_0 - q\lambda M^{12}(0) + \mu M^{13}(0), \tag{1.15}$$

$$\bar{E}_1 = \lambda M^{12}(1) - M^{14}E_1 - \rho\mu M^{13}(1), \tag{1.16}$$

$$M_1 = -M^{14}\bar{A}_{11} + A_0 M^{14} + E_0 M^{34}(0), \tag{1.17}$$

$$M_p = -M^{15}A_{22} - M^{14}\bar{A}_{12} + A_0 M^{15} + E_0 M^{35}(0), \tag{1.18}$$

$$M^{\alpha}(y) = -\lambda \frac{\mathrm{d}}{\mathrm{d}y} M^{12}(y) + A_0 M^{12}(y) + E_0 M^{32}(0, y), \tag{1.19}$$

$$M^{\beta}(y) = \mu \frac{\mathrm{d}}{\mathrm{d}y} M^{13}(y) + A_0 M^{13}(y) + E_0 M^{33}(0, y). \tag{1.20}$$

The initial conditions $(\xi_0, \alpha_0, \beta_0, \eta_0) \in \mathcal{X}$ are defined from the initial conditions of the system (1.1)-(1.6) using the integral transform. The different coefficients naturally derive from the backstepping procedure. We also define a new actuation $\tilde{U}(t) \doteq U(t) - F_0\xi(t)$ in (1.11), with F_0 defined in Assumption 2. Note that in absence of disturbance, namely $\eta_2 \equiv 0$, this target system was shown to be stabilizable in [8].

1.3.3 Kernel equations

Following the backstepping procedure, we derive equations (1.9)-(1.10) and integrate by parts to find the equations satisfied by the different kernels defined on $\mathcal{T}^+$. We obtain

$$\lambda M_x^{22}(x, y) + \lambda M_y^{22}(x, y) = \sigma^+(x) M^{32}(x, y), \tag{1.21}$$

$$\lambda M_x^{23}(x, y) - \mu M_y^{23}(x, y) = \sigma^+(x) M^{33}(x, y), \tag{1.22}$$

$$\mu M_x^{32}(x, y) - \lambda M_y^{32}(x, y) = -\sigma^-(x) M^{22}(x, y), \tag{1.23}$$

$$\mu M_x^{33}(x, y) + \mu M_y^{33}(x, y) = -\sigma^-(x) M^{23}(x, y), \tag{1.24}$$

with the boundary conditions

$$M^{23}(x, x) = -\frac{\sigma^+(x)}{\lambda + \mu}, \quad M^{32}(x, x) = \frac{\sigma^-(x)}{\lambda + \mu}, \tag{1.25}$$

$$M^{22}(x, 1) = \frac{1}{\lambda}\left(M^{24}(x)E_1 + \rho\mu M^{23}(x, 1)\right), \tag{1.26}$$

$$M^{33}(x, 1) = \frac{1}{\mu\rho}\left(\lambda M^{32}(x, 1) - M^{34}(x)E_1\right). \tag{1.27}$$

The kernels associated to the state $\eta(t)$ are defined on $[0, 1]$ and must satisfy the set of ODEs

$$\lambda \frac{\mathrm{d}}{\mathrm{dx}} M^{24}(x) + M^{24}(x)\bar{A}_{11} = \sigma^{+}(x)M^{34}(x), \tag{1.28}$$

$$\lambda \frac{\mathrm{d}}{\mathrm{dx}} M^{25}(x) + M^{25}(x)A_{22} = \sigma^{+}(x)M^{35}(x) - M^{24}(x)\bar{A}_{12}, \tag{1.29}$$

$$\mu \frac{\mathrm{d}}{\mathrm{dx}} M^{34}(x) - M^{34}(x)\bar{A}_{11} = -\sigma^{-}(x)M^{24}(x), \tag{1.30}$$

$$\mu \frac{\mathrm{d}}{\mathrm{dx}} M^{35}(x) - M^{35}(x)A_{22} = -\sigma^{-}(x)M^{25}(x) + M^{34}(x)\bar{A}_{12}, \tag{1.31}$$

with the boundary conditions

$$M^{24}(1) = F_1, \quad M^{25}(1) = F_a + F_1 T_a, \tag{1.32}$$

$$M^{34}(1) = C_{11} + \rho F_1, \quad M^{35}(1) = C_{12} + \rho M^{25}(1), \tag{1.33}$$

where F_1 is defined by Assumption 2 and (F_a, T_a) is defined by Assumption 4. Finally, the following set of algebraic relations is fulfilled

$$C_0 M^{12}(y) = M^{22}(0,y) - qM^{32}(0,y), \tag{1.34}$$

$$C_0 M^{13}(y) = M^{23}(0,y) - qM^{33}(0,y), \tag{1.35}$$

$$C_0 M^{14} = M^{24}(0) - qM^{34}(0), \tag{1.36}$$

$$C_0 M^{15} = M^{25}(0) - qM^{35}(0). \tag{1.37}$$

The kernels are well-defined on their definition domain.

1.3.4 frequency analysis of the target system

Let us denote $\tau = \frac{1}{\mu} + \frac{1}{\lambda}$. We use the method of characteristics to rewrite the target system as a *time-delay system*. Then, we analyze the properties of such system in the frequency domain. We express the Laplace transform of $\alpha(\cdot,0), \beta(\cdot,1)$ and η_1 in function of the ones of η_2, ξ. After some technical computations, we finally obtain for any $s \in \mathbb{C}$ with $\mathrm{Re}(s) \geq 0$

$$(sI - \bar{A}_0)\mathscr{L}(\xi)(s) = G(s)C_0\mathscr{L}(\xi)(s) + H(s)\mathscr{L}(\eta_2)(s) + B_0\mathscr{L}(\tilde{U})(s), \tag{1.38}$$

with

$$G(s) = -\lambda M^{12}(0) \tag{1.39}$$

$$+(1-\rho q \mathrm{e}^{-\tau s})^{-1}\left[\left(\bar{E}_1 + M_1(sI - \bar{A}_{11})^{-1}E_1\right)\mathrm{e}^{-\frac{s}{\lambda}} + \rho \mathrm{e}^{-\tau s}\bar{E}_0 + \int_0^{\tau} M^{\xi}(\theta)\mathrm{e}^{-s\theta}\mathrm{d}\theta\right],$$

$$M^{\xi}(\theta) = \lambda M^{\alpha}(\lambda\theta)\mathbb{1}_{[0,\frac{1}{\lambda}]}(\theta) + \rho\mu M^{\beta}\left(1 - \mu\theta + \frac{\mu}{\lambda}\right)\mathbb{1}_{(\frac{1}{\lambda},\tau]}(\theta), \tag{1.40}$$

$$H(s) = M_1(sI - \bar{A}_{11})^{-1}\bar{A}_{12} + M_p. \tag{1.41}$$

This will be further used in the design of the control law stabilizing $\epsilon(t)$. In the next section, we use the transfer functions we defined to determine an adequate input $\tilde{U}(t)$, corresponding to $\mathscr{L}(\tilde{U})(s)$ in the Laplace domain.

1.3.5 Full-state feedback controller design

We now design a control law for the practical output regulation of the target system $(\xi, \alpha, \beta, \eta)$, and more precisely its Laplace transform $\mathscr{L}(\tilde{U})(s)$. It is decomposed into two parts: $\mathscr{L}(\tilde{U})(s) = U_\xi(s) + U_\eta(s)$. First, we design a stabilizing state feedback control law U_ξ for the system in absence of the disturbance or reference signal (i.e $\eta_2 = Y_2 \equiv 0$), using the results from [8]. Then, we design a robust bounded control law U_η depending on the dynamics of the perturbation, to cancel its effects on the dynamics of ξ. The practical output tracking/output regulation problems are therefore solved.

1.3.5.1 Target system stabilization in absence of disturbance

Following the procedure in [8] for the extended system, we design a state feedback control law of form $U_\xi(s) = F_\xi(s) C_0 \mathscr{L}(\xi)(s)$ stabilizing the output $C_0\xi(.)$. It implies the stabilization of the target system.
When $\eta_2 \equiv 0$, (1.38) rewrites on the complex right half plane

$$C_0\mathscr{L}(\xi)(s) = C_0(sI - \bar{A}_0)^{-1}G(s)C_0\mathscr{L}(\xi)(s) + P_0\mathscr{L}(\tilde{U})(s), \tag{1.42}$$

with P_0 defined in Assumption 3. As previously mentioned, $P_0(s)$ admits a stable right inverse $P_0^+(s)$, for instance the Moore-Penrose right inverse $P_0^+(s) \doteq P_0^T(s)(P_0(s)P_0^T(s))^{-1}$.
We now define the transfer function $F_\xi(s) = -P_0^+(s)C_0(sI - \bar{A}_0)^{-1}G(s)$. Since it is not necessarily proper, we can use a filtering technique as in [8].
Let us decompose $G(s)$ in (1.39) into $G(s) = \mathrm{w}(s)G(s) + (1 - \mathrm{w}(s))G(s)$, with $\mathrm{w}(s)$ a (SISO) stable low-pass filter of sufficient order. A candidate (proper) controller can therefore be defined as

$$\tilde{F}_\xi(s) = -P_0^+(s)\left[C_0(sI - \bar{A}_0)^{-1}\mathrm{w}(s)G(s)\right]. \tag{1.43}$$

We have the following theorem [8]:

Lemma 1 *Let* $\mathrm{w}(s)$ *be any low-pass filter, with sufficiently high relative degree, and* $0 < \delta < 1$ *sufficiently small, such that*

$$\forall x \in \mathbb{R},\ |1 - \mathrm{w}(jx)| \leq \frac{1-\delta}{\|G\|_\infty \bar{\sigma}(C_0(jxI - \bar{A}_0)^{-1})}. \tag{1.44}$$

Then the dynamic output feedback $\tilde{U}_\xi(s) = \tilde{F}_\xi(s)C_0\mathscr{L}(\xi)(s)$ *with* $\tilde{F}_\xi(s)$ *given in* (1.43) *exponentially stabilizes* $C_0\xi(.)$.

Proof The proof is omitted here due to space restriction. More details are given in [8].

Then, let us show that the target system is exponentially stabilized by the state feedback (1.43).

Theorem 1 *Assume that* $C_0\xi(\cdot)$ *is exponentially stabilized by a dynamic output feedback of the form* $U_\xi(s) = F_\xi(s)C_0\mathscr{L}(\xi)(s)$ *where* $F_\xi(s)$ *is a stable strictly-proper transfer matrix. Then, under Assumptions 1-3, the target system* (1.11)-(1.14) *in absence of perturbation is exponentially stable in the* $\mathcal{X}$*-norm.*

Proof The proof is omitted here due to space restriction.

Using Lemma 1 and Theorem 1, we have designed a stabilizing control input $\tilde{U}$ for the target system. We can then deduce the corresponding control input for the original system (1.1)-(1.5) as $U(t) = \tilde{U}(t) + F_0\xi(t)$.

1.3.5.2 Practical output regulation

Following the same procedure, we can now design a control law based on the supposedly known perturbation to cancel the effects of the disturbance η_2 on the dynamics of the output $C_0\xi(.)$.
In presence of perturbation, (1.38) rewrites for any $s \in \mathbb{C}$ with $\mathrm{Re}(s) \geq 0$

$$\begin{aligned} C_0\mathscr{L}(\xi)(s) = \; & C_0(sI - \bar{A}_0)^{-1}G(s)C_0\mathscr{L}(\xi)(s) + P_0(s)U_\xi(s) \\ & + C_0(sI - \bar{A}_0)^{-1}H(s)\mathscr{L}(\eta_2)(s) + P_0(s)U_\eta(s). \end{aligned} \tag{1.45}$$

First, let us define the transfer function $F_\eta(s) \doteq -P_0^+(s)C_0(sI - \bar{A}_0)^{-1}H(s)$, s.t. knowing the perturbation, the control law $U_\eta(s) = F_\eta(s)\mathscr{L}(\eta_2)(s)$ cancels the effect of the perturbation on the target system.
As above, since the obtained transfer function is not proper in general, we can regularize it to design a strictly proper transfer function

$$\tilde{F}_\eta(s) = -P_0^+(s)C_0(sI - \bar{A}_0)^{-1}H(s)w(s), \tag{1.46}$$

using an adequately chosen low-pass filter $w(s)$. We now show the following theorem:

Theorem 2 *Assume that in the absence of the disturbance, the function* $C_0\mathscr{L}(\xi)(s)$ *is exponentially stabilized by a dynamic full-state feedback of the form* $\tilde{U}_\xi(s) = \tilde{F}_\xi(s)C_0\mathscr{L}(\xi)(s)$. *Consider the extended control law*

$$\mathscr{L}(U)(s) = (\tilde{F}_\xi(s)C_0 + F_0)\mathscr{L}(\xi)(s) + \tilde{F}_\eta(s)\mathscr{L}(\eta_2)(s), \tag{1.47}$$

where $\tilde{F}_\xi(s), \tilde{F}_\eta(s)$ are two stable (proper) transfer matrices. Then, under Assumptions 1, 2, 3, 4, the virtual output $\epsilon(t)$ is practically regulated to zero. This is, given the norm of the initial condition of the exosystem $\eta_2(0)$, and given a desired asymptotic bound for the virtual output $\epsilon(t)$ ($\equiv$ tracking error), we can choose an adequate low-pass filter $w(s)$ such that the practical tracking objective is attained. Furthermore, under these assumptions, the control action and the trajectories of ξ and η remain bounded.

Proof In the absence of disturbances or tracking signals, the state of the system converges exponentially to zero, due to the exponential stability of $C_0\mathscr{L}(\xi)(s)$. Since the disturbance signal remains bounded (Assumption 4), so does the state in presence of the disturbance (or reference trajectory) term. More precisely, with the control law (1.47), we have

$$\begin{aligned} &C_0\mathscr{L}(\xi)(s) = C_0(sI - \bar{A}_0)^{-1}(1 - w(s))(G(s)C_0\mathscr{L}(\xi)(s) + H(s)\mathscr{L}(\eta_2)(s)) \\ &\implies (1 - \Phi(s))C_0\mathscr{L}(\xi)(s) = C_0(sI - \bar{A}_0)^{-1}(1 - w(s))H(s)\mathscr{L}(\eta_2)(s)). \end{aligned}$$

The gain between the disturbance or trajectory term and the residual term $C_0\mathscr{L}(\xi)(s)$ can be chosen to be arbitrarily small at the frequencies contained in the disturbance or trajectories, in order to guarantee that the virtual output $\epsilon(t)$ converges practically to zero.
The stability of $\alpha(\cdot,0)$, $\beta(\cdot,1)$ is deduced from the Laplace transform of (1.14), which implies a bounded gain between the exo-system state (reference/reference trajectory) and α and β in the L^2-norm.
Let us now study the behaviour of $C_{e1}\eta_1 + C_{e2}\eta_2$ in the absence of disturbances or reference trajectories. The dynamics of η_1 rewrites

$$\begin{aligned} \dot{\eta}_1(t) &= (A_{11} + E_1F_1)\eta_1(t) + A_{12}\eta_2(t) + E_1(F_a + F_1T_a)\eta_2(t) + E_1\alpha(t,1), \\ &= (A_{11} + E_1F_1)\eta_1(t) + (-E_1F_a + A_{11}T_a - T_aA_{22})\eta_2(t) \\ &\quad + E_1(F_a + F_1T_a)\eta_2(t) + E_1\alpha(t,1) \quad \text{by Assumption 4} \\ &\implies \dot{(\eta_1 + T_a\eta_2)}(t) = \bar{A}_{11}(\eta_1 + T_a\eta_2) + \underbrace{E_1\alpha(t,1)}_{\longrightarrow 0}. \end{aligned} \tag{1.48}$$

Therefore, the dynamics of $\eta_1 + T_a\eta_2$ is stable. It implies that $C_{e1}(\eta_1 + T_a\eta_2)(t) = C_{e1}(Y_1 + T_aY_2)(t) = C_{e1}Y_1(t) + C_{e2}Y_2(t) = \epsilon(t)$ has a bounded gain w.r.t. $\alpha(t,1)$. If, $\alpha(t,1)$ converges to an arbitrarily small value (selected by adequately choosing the low-pass filter $w(s)$), then, $C_{e1}\eta_1 + C_{e2}\eta_2$ can be made to converge to a desired neighborhood of zero.

Theorem 2 proves that there exists a dynamic feedback in the form (1.47), the parameters of which can be chosen depending only on the norm of the exo-system state and the desired precision for the tracking, such that the virtual output $\epsilon(t)$ converges to any desired neighborhood of zero. Given the control input $\tilde{U}$ for the target system, the corresponding control input for the original system can be obtained $U(t) = \tilde{U}(t) + F_0\xi(t)$.

Remark that the controller has been chosen as strictly proper which means that it is robust to small delays in the input, which is not the case in some designs that include derivative terms. The proof follows the same ideas as those in [4].
In the case where the exogenous state $Y_2(t) = \eta_2(t)$ is a reference trajectory supposedly known, we can make the output $\epsilon(t)$ converge arbitrarily close to zero knowing the evolution of $\xi(t)$ using the robust full-state feedback control law $U(t) = U_\xi(t) + U_\eta(t) + F_0\xi(t)$. However, this full-state feedback controller requires the knowledge of all the states (X,u,v,Y) at any time. For further applications on real systems, it is then necessary to *estimate* the state (X,u,v,Y) using the measure $y(t)$.

In the case where the exogenous state Y_2 is an unknown disturbance, the control law we propose is not fully satisfactory. We need to reconstruct the perturbation since the knowledge of η_2 is required to design the control law $U(t)$.

1.4 Output dynamic feedback controller design

In this section, we first use the backstepping approach to map the original system (1.1)-(1.6) to a simpler target system, for which we design an observer. Following [13], we use an invertible transform to map the error system to a stable target system and design the corresponding observer gains. Next, we integrate the observers in the previously designed control law to obtain an output-feedback controller solving the practical output tracking/output regulation problem.

1.4.1 Observer design

We now design an adequate invertible transform to map system (1.1)-(1.6) to a simpler target system, as schematized on Figure 1.3.

1.4.1.1 Invertible transform and target system

In order to map the initial system (1.1)-(1.6) to an simpler target system, we use the following backstepping transform

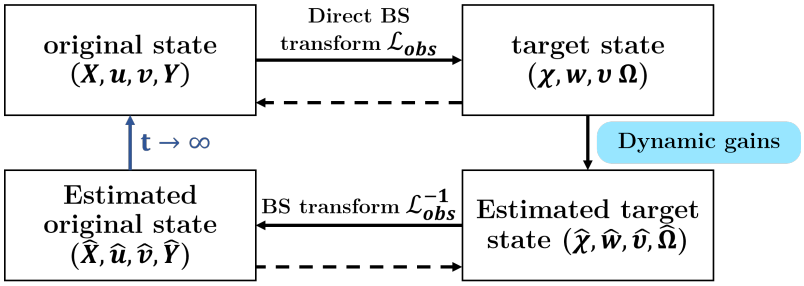

Fig. 1.3 Observer design strategy for system (1.1)-(1.6)

$$X(t) = \chi(t), \tag{1.49}$$

$$u(t,x) = w(t,x) + \int_0^x L^{22}(x,y)w(y) + L^{23}(x,y)v(y)\mathrm{d}y, \tag{1.50}$$

$$v(t,x) = v(t,x) + \int_0^x L^{32}(x,y)w(y) + L^{33}(x,y)v(y)\mathrm{d}y, \tag{1.51}$$

$$Y(t) = \Omega(t) + \int_0^1 \begin{bmatrix} L^{42} \\ L^{52} \end{bmatrix}(y)w(y) + \begin{bmatrix} L^{43} \\ L^{53} \end{bmatrix}(y)v(y)\mathrm{d}y, \tag{1.52}$$

where the kernel functions $L^{i2}, L^{i3} \in C([0,1];\mathbb{R}^{*\times 1})$ ($* = m$ if $i = 4$, $* = p$ if $i = 5$) and $L^{22}, L^{23}, L^{32}, L^{33} \in C(\mathcal{T}^-;\mathbb{R})$ have yet to be defined. For the same reasons given in section 1.3.1, this transform is invertible. The inverse transform $\mathcal{L}_{\text{obs}}$ (with direct formulation) has the same structure that the transform (1.49)-(1.52) with kernels N^{ij} being expressed as functions of L^{ij}.

Let us define a target state denoted $(\chi, w, v, \Omega) \in \mathcal{X}$, where $\Omega(t) = \begin{bmatrix}\Omega_1(t) & \Omega_p(t)\end{bmatrix}^T$ is decomposed into two parts. This new set of variables satisfies

$$\dot{\chi}(t) = A_0\chi(t) + E_0 v(t,0) + B_0 U(t), \tag{1.53}$$

$$w_t(t,x) + \lambda w_x(t,x) = g_w(x)v(t,0) + h_w(x)\chi(t), \tag{1.54}$$

$$v_t(t,x) - \mu v_x(t,x) = g_v(x)v(t,0) + h_v(x)\chi(t), \tag{1.55}$$

$$\dot{\Omega}(t) = A_1^{\text{obs}}\Omega(t) + K_\Omega^{v,0}v(t,0) + K_\Omega^{\chi}\chi(t), \tag{1.56}$$

with the boundary conditions

$$w(t,0) = qv(t,0) + C_0\chi(t), \quad v(t,1) = \rho w(t,1) + \begin{bmatrix} C_{11} & C_{12} \end{bmatrix}\Omega(t), \tag{1.57}$$

where A_1^{obs} is defined by Assumption 5. The different coefficients naturally derive from the backstepping procedure. The functions g_w, g_v are defined by

the set of integral equations[1]

$$g_w(x) + \int_0^x L^{22}(x,y)g_w(y) + L^{23}(x,y)g_\upsilon(y)\mathrm{d}y = \mu L^{23}(x,0) - \lambda q L^{22}(x,0),$$
$$g_\upsilon(x) + \int_0^x L^{32}(x,y)g_w(y) + L^{33}(x,y)g_\upsilon(y)\mathrm{d}y = \mu L^{33}(x,0) - \lambda q L^{32}(x,0),$$

and the functions h_w, h_υ by

$$h_w(x) + \int_0^x L^{22}(x,y)h_w(y) + L^{23}(x,y)h_\upsilon(y)\mathrm{d}y = -\lambda L^{22}(x,0)C_0,$$
$$h_\upsilon(x) + \int_0^x L^{32}(x,y)h_w(y) + L^{33}(x,y)h_\upsilon(y)\mathrm{d}y = -\lambda L^{32}(x,0)C_0.$$

These coupled integral equations admit a unique solution [26]. The terms $K_\Omega^{\upsilon,0}, K_\Omega^{\chi}$ are defined by

$$K_\Omega^{\upsilon,0} = \mu \begin{bmatrix} L^{43}(0) \\ L^{53}(0) \end{bmatrix} - \lambda q \begin{bmatrix} L^{42}(0) \\ L^{52}(0) \end{bmatrix} - \int_0^1 \begin{bmatrix} L^{42}(y) \\ L^{52}(y) \end{bmatrix} g_w(y) + \begin{bmatrix} L^{43}(y) \\ L^{53}(y) \end{bmatrix} g_\upsilon(y)\mathrm{d}y,$$
$$K_\Omega^{\chi} = -\lambda \begin{bmatrix} L^{42}(0) \\ L^{52}(0) \end{bmatrix} C_0 - \int_0^1 \begin{bmatrix} L^{42}(y) \\ L^{52}(y) \end{bmatrix} h_w(y) + \begin{bmatrix} L^{43}(y) \\ L^{53}(y) \end{bmatrix} h_\upsilon(y)\mathrm{d}y.$$

1.4.1.2 Kernel equations

We derive equations (1.53)-(1.56) and integrate by parts to find the equations satisfied by the kernels L^{ij} on their definition domain. The equations in w, υ imply that kernels $L^{22}, L^{23}, L^{32}, L^{33}$ are defined by the following set of PDEs

$$\lambda L_x^{22}(x,y) + \lambda L_y^{22}(x,y) = \sigma^+(x)L^{32}(x,y), \tag{1.58}$$
$$\lambda L_x^{23}(x,y) - \mu L_y^{23}(x,y) = \sigma^+(x)L^{33}(x,y), \tag{1.59}$$
$$\mu L_x^{32}(x,y) - \lambda L_y^{32}(x,y) = -\sigma^-(x)L^{22}(x,y), \tag{1.60}$$
$$\mu L_x^{33}(x,y) + \mu L_y^{33}(x,y) = -\sigma^-(x)L^{23}(x,y), \tag{1.61}$$

with the boundary conditions

[1] Note that an explicit expression of g_w, g_υ could have been obtained using the transform $\mathcal{L}_{\mathrm{obs}}$ with direct formulation. However, it would have led to more complex terms in the boundary conditions (1.57).

$$L^{23}(x,x) = \frac{\sigma^+(x)}{\lambda+\mu}, \quad L^{32}(x,x) = -\frac{\sigma^-(x)}{\lambda+\mu}, \tag{1.62}$$

$$L^{22}(1,y) = \frac{1}{\rho}(L^{32}(1,y) - \begin{bmatrix} C_{11} & C_{12} \end{bmatrix} \begin{bmatrix} L^{42}(y) \\ L^{52}(y) \end{bmatrix}), \tag{1.63}$$

$$L^{33}(1,y) = \rho L^{23}(1,y) + \begin{bmatrix} C_{11} & C_{12} \end{bmatrix} \begin{bmatrix} L^{43}(y) \\ L^{53}(y) \end{bmatrix}. \tag{1.64}$$

The equations in Ω imply that $L^{42}, L^{43}, L^{52}, L^{53}$ satisfy the following set of ODEs

$$\lambda \frac{\mathrm{d}}{\mathrm{d}y} \begin{bmatrix} L^{42} \\ L^{52} \end{bmatrix}(y) = \begin{bmatrix} A_{11} & A_{12} \\ 0_{p\times m} & A_{22} \end{bmatrix} \begin{bmatrix} L^{42} \\ L^{52} \end{bmatrix}(y) + \begin{bmatrix} E_1 \\ 0_{p\times 1} \end{bmatrix} L^{22}(1,y), \tag{1.65}$$

$$-\mu \frac{\mathrm{d}}{\mathrm{d}y} \begin{bmatrix} L^{43} \\ L^{53} \end{bmatrix}(y) = \begin{bmatrix} A_{11} & A_{12} \\ 0_{p\times m} & A_{22} \end{bmatrix} \begin{bmatrix} L^{43} \\ L^{53} \end{bmatrix}(y) + \begin{bmatrix} E_1 \\ 0_{p\times 1} \end{bmatrix} L^{23}(1,y), \tag{1.66}$$

with the boundary conditions

$$\begin{bmatrix} L^{42} \\ L^{52} \end{bmatrix}(1) = -\frac{1}{\lambda}(\rho \begin{bmatrix} L_1 \\ L_2 \end{bmatrix} + \begin{bmatrix} E_1 \\ 0_{p\times 1} \end{bmatrix}), \quad \begin{bmatrix} L^{43} \\ L^{53} \end{bmatrix}(1) = -\frac{1}{\mu} \begin{bmatrix} L_1 \\ L_2 \end{bmatrix}, \tag{1.67}$$

with $\begin{bmatrix} L_1 \\ L_2 \end{bmatrix}$ defined by Assumption 5.

The kernels are well-defined on their domains of definition. More precisely, we simultaneously solve the set of coupled PDEs and ODEs $L^{22}, L^{23}, L^{32}, L^{33}$ and $L^{42}, L^{43}, L^{52}, L^{53}$. Indeed, the kernels $L^{42}, L^{43}, L^{52}, L^{53}$ can be *embedded* onto the triangular domain $\mathcal{T}^+$, by defining $\tilde{L}^{ij}(x,y) \doteq \mathbb{1}_{x=1}(x,y)L^{ij}(x)$, $i \in \{2,3\}$, $j \in \{4,5\}$. Following the proof of the main result from [12], stating the existence of a solution of a general class of kernel equations, we conclude that (1.58)-(1.67) admits a unique L^∞ solution. Higher regularity can be obtained by following the same procedure and requiring higher regularity in the coefficients.

1.4.1.3 Observer and error state

We recall that we have access to the measurement $y(t) = C_{\mathrm{mes}}X(t) = C_{\mathrm{mes}}\chi(t) \in \mathbb{R}^{n'}$. We introduce the observer state system as a copy of the target dynamics, with dynamic output feedback gains $\mathcal{P}_\cdot$, the structure of which will be precised later this section.

$$\dot{\hat{\chi}}(t) = A_0\hat{\chi}(t) + E_0\hat{\upsilon}(t,0) + B_0U(t) - P_\chi\left(y(t) - C_{\mathrm{mes}}\hat{\chi}(t)\right), \tag{1.68}$$

$$\hat{w}_t(t,x) + \lambda\hat{w}_x(t,x) = g_w(x)\hat{\upsilon}(t,0) + h_w(x)\hat{\chi}(t) - \mathcal{P}_w(t,x), \tag{1.69}$$

$$\hat{\upsilon}_t(t,x) - \mu\hat{\upsilon}_x(t,x) = g_\upsilon(x)\hat{\upsilon}(t,0) + h_\upsilon(x)\hat{\chi}(t) - \mathcal{P}_\upsilon(t,x), \tag{1.70}$$

$$\dot{\hat{\Omega}}(t) = A_1^{\mathrm{obs}}\hat{\Omega}(t) + K_\Omega^{\upsilon,0}\hat{\upsilon}(t,0) + K_\Omega^{\chi}\hat{\chi}(t) - \mathcal{P}_\Omega(t), \tag{1.71}$$

with boundary conditions

$$\hat{w}(t,0) = q\hat{\upsilon}(t,0) + C_0\hat{\chi}(t) - \mathcal{P}_w^0(t),\ \hat{\upsilon}(t,1) = \rho\hat{w}(t,1) + \begin{bmatrix} C_{11} & C_{12} \end{bmatrix}\hat{\Omega}(t) \tag{1.72}$$

with any initial conditions in $\mathcal{X}$. The observer gain P_χ and injected signals $\mathcal{P}_w, \mathcal{P}_\upsilon, \mathcal{P}_\Omega, \mathcal{P}_w^0$ will be chosen to stabilize the error system, whose state is defined by $(\tilde{\chi}, \tilde{w}, \tilde{\upsilon}, \tilde{\Omega}) \doteq (\chi, w, \upsilon, \Omega) - (\hat{\chi}, \hat{w}, \hat{\upsilon}, \hat{\Omega})$.
The error state satisfies the set of equations

$$\dot{\tilde{\chi}}(t) = A_0\tilde{\chi}(t) + E_0\tilde{\upsilon}(t,0) + P_\chi C_{\text{mes}}\tilde{\chi}(t), \tag{1.73}$$
$$\tilde{w}_t(t,x) + \lambda\tilde{w}_x(t,x) = g_w(x)\tilde{\upsilon}(t,0) + h_w(x)\tilde{\chi}(t) + \mathcal{P}_w(t,x), \tag{1.74}$$
$$\tilde{\upsilon}_t(t,x) - \mu\tilde{\upsilon}_x(t,x) = g_\upsilon(x)\tilde{\upsilon}(t,0) + h_\upsilon(x)\tilde{\chi}(t) + \mathcal{P}_\upsilon(t,x), \tag{1.75}$$
$$\dot{\tilde{\Omega}}(t) = A_1^{\text{obs}}\tilde{\Omega}(t) + K_\Omega^{\upsilon,0}\tilde{\upsilon}(t,0) + K_\Omega^{\chi}\tilde{\chi}(t) + \mathcal{P}_\Omega(t), \tag{1.76}$$

with the boundary conditions

$$\tilde{w}(t,0) = q\tilde{\upsilon}(t,0) + C_0\tilde{\chi}(t) + \mathcal{P}_w^0(t), \tag{1.77}$$
$$\tilde{\upsilon}(t,1) = \rho\tilde{w}(t,1) + \begin{bmatrix} C_{11} & C_{12} \end{bmatrix}\tilde{\Omega}(t). \tag{1.78}$$

First, we can define $P_\chi \doteq L_X$, with L_X given in Assumption 5, such that (1.73) rewrites $\dot{\tilde{\chi}}(t) = A_0^{\text{obs}}\tilde{\chi}(t) + E_0\tilde{\upsilon}(t,0)$.

1.4.1.4 Frequency analysis of the error system

In this section, we determine the functions $\mathcal{P}_w, \mathcal{P}_\upsilon, \mathcal{P}_\Omega, \mathcal{P}_w^0$ to ensure the stability of the error system (1.73)-(1.78) in the sense of the $\mathcal{X}-$norm. The Laplace transform of (1.73) gives

$$\begin{aligned} (sI - A_0^{\text{obs}})\mathscr{L}(\tilde{\chi})(s) &= E_0\mathscr{L}(\tilde{\upsilon}(.,0))(s) \\ \implies \mathscr{L}(\tilde{\chi})(s) &= (sI - A_0^{\text{obs}})^{-1}E_0\mathscr{L}(\tilde{\upsilon}(.,0))(s) \quad \forall s \in \mathbb{C}^+, \end{aligned} \tag{1.79}$$

since $sI - A_0^{\text{obs}}$ is non-singular on the complex right-half plane by Assumption 5.
Then, let us determine the signals $\mathcal{P}_w(t,x), \mathcal{P}_\upsilon(t,x)$. Applying the variation of constants formula in (1.74)-(1.75), we have

$$\tilde{w}(t,1) = \tilde{w}(t-\frac{1}{\lambda},0) + \int_0^{\frac{1}{\lambda}} g_w(1-\lambda\theta)\tilde{v}(t-\theta,0) + h_w(1-\lambda\theta)\tilde{\chi}(t-\theta) + \mathcal{P}_w(t-\theta,1-\lambda\theta)\mathrm{d}\theta, \tag{1.80}$$

$$\tilde{v}(t,0) = \tilde{v}(t-\frac{1}{\mu},0) + \int_0^{\frac{1}{\mu}} g_v(\mu\theta)\tilde{v}(t-\theta,0) + h_v(\mu\theta)\tilde{\chi}(t-\theta) + \mathcal{P}_v(t-\theta,\mu\theta)\mathrm{d}\theta. \tag{1.81}$$

Taking the Laplace transform of (1.80), and incorporating therein the Laplace transform of $\tilde{\chi}$ deduced from (1.79), we have

$$\mathscr{L}(\tilde{w}(.,1))(s) = e^{-\frac{s}{\lambda}}\mathscr{L}(\tilde{w}(.,0))(s) + \int_0^{\frac{1}{\lambda}} (g_w(1-\lambda\theta) + h_w(1-\lambda\theta)(sI - A_0^{\mathrm{obs}})^{-1}E_0)\mathscr{L}(\tilde{v}(.,0))(s) + \mathcal{P}_w(s,1-\lambda\theta))e^{-s\theta}\mathrm{d}\theta. \tag{1.82}$$

Assume we have a gain $\mathcal{P}_w$ of the form $\mathcal{P}_w(s,x) = P_w(s,x)C_{\mathrm{mes}}\mathscr{L}(\tilde{\chi})(s)$, with $x = 1-\lambda\theta \in [0,1]$. By (1.79), this implies $\mathcal{P}_w(s,x) = P_w(s,x)P_{\mathrm{mes}}(s)\mathscr{L}(\tilde{v}(.,0))(s)$ for all $s \in \mathbb{C}^+$, with $P_{\mathrm{mes}}(s)$ defined after Assumption 6. This transfer function admits a stable left-inverse denoted $P_{\mathrm{mes}}^-(s)$ (which is not necessarily proper). In our examples, we will use the Moore-Penrose left inverse

$$P_{\mathrm{mes}}^-(s) \doteq (P_{\mathrm{mes}}^T(s)P_{\mathrm{mes}}(s))^{-1}P_{\mathrm{mes}}^T(s)$$

which is verified to be stable. In order to rewrite (1.74) as a transport equation, that is to say, in the Laplace domain, $\mathscr{L}(\tilde{w}(.,1))(s) = e^{-\frac{s}{\lambda}}\mathscr{L}(\tilde{w}(.,0))(s)$, we thus define the transfer function

$$P_w(s,x) \doteq -(g_w(x) + h_w(x)(sI - A_0^{\mathrm{obs}})^{-1}E_0)P_{\mathrm{mes}}^-(s). \tag{1.83}$$

Similarly, taking the Laplace transform of (1.81), and incorporating therein the Laplace expression (1.79), we have

$$\mathscr{L}(\tilde{v}(.,0))(s) = e^{-\frac{s}{\mu}}\mathscr{L}(\tilde{v}(.,1))(s) + \int_0^{\frac{1}{\mu}} (g_v(\mu\theta) + h_v(\mu\theta)(sI - A_0^{\mathrm{obs}})^{-1}E_0)\mathscr{L}(\tilde{v}(.,0))(s) + \mathcal{P}_v(s,\mu\theta))e^{-s\theta}\mathrm{d}\theta.$$

In order to rewrite (1.75) as a transport equation, that is to say, in the Laplace domain, $\mathscr{L}(\tilde{v}(.,0))(s) = e^{-\frac{s}{\mu}}\mathscr{L}(\tilde{v}(.,1))(s)$, we can choose the observer gain of form $\mathcal{P}_v(s,x) = P_v(s,x)C_{\mathrm{mes}}\mathscr{L}(\tilde{\chi})(s)$. To cancel the terms in the integral, we thus define

$$P_v(s,x) \doteq -(g_v(x) + h_v(x)(sI - A_0^{\mathrm{obs}})^{-1}E_0)P_{\mathrm{mes}}^-(s). \tag{1.84}$$

In order to guarantee that for all $x \in [0,1]$, $P_w(s,x), P_v(s,x)$ are strictly proper transfer functions, it is still possible to use an adequate low-pass filter $\omega(s)$ of sufficient order. Taking the Laplace transform of (1.77) and incorporating

therein (1.79), we have $\mathscr{L}(\tilde{w}(.,0))(s)(q + C_0(sI - A_0^{\text{obs}})^{-1}E_0)\ \mathscr{L}(\tilde{\upsilon}(.,0))(s) + \mathcal{P}_w^0(s)$. Therefore, choosing $\mathcal{P}_w^0(s)$ of the form $\mathcal{P}_w^0(s) \doteq P_w^0(s)C_{\text{mes}}\mathscr{L}(\tilde{\chi})(s)$, we define the transfer function

$$P_w^0(s) \doteq -(q + C_0(sI - A_0^{\text{obs}})^{-1}E_0)P_{\text{mes}}^-(s), \tag{1.85}$$

such that the reflection terms at the boundary are cancelled.[2] Finally, taking the Laplace transform of (1.76) and incorporating therein (1.79), we have

$$(sI - A_1^{\text{obs}})\mathscr{L}(\tilde{\Omega})(s) = (K_\Omega^{\upsilon,0} + K_\Omega^{\chi}(sI - A_0^{\text{obs}})^{-1}E_0)\mathscr{L}(\tilde{\upsilon}(.,0))(s) + \mathcal{P}_\Omega(s),$$

with $sI - A_1^{\text{obs}}$ non-singular on the right half plane due to Assumption 5. Once again, we assume we have a signal of the form $\mathcal{P}_\Omega(s) = P_\Omega(s)\ C_{\text{mes}}\mathscr{L}(\tilde{\chi})(s)$. In order to guarantee the convergence of $\tilde{\Omega}$ to zero, we consequently define

$$P_\Omega(s) = -(K_\Omega^{\upsilon,0} + K_\Omega^{\chi}(sI - A_0^{\text{obs}})^{-1}E_0)P_{\text{mes}}^-(s). \tag{1.86}$$

Again, since $P_{\text{mes}}^-(s)$ is not necessarily proper, we can use the low-pass filter $\omega(s)$ to filter all the transfer functions. In the following, we describe the construction of a stabilizing output feedback of form

$$\mathcal{P}_w(s,\theta) = \omega(s)P_w(s,\theta)C_{\text{mes}}\mathscr{L}(\tilde{\chi})(s), \tag{1.87}$$
$$\mathcal{P}_\upsilon(s,\theta) = \omega(s)P_\upsilon(s,\theta)C_{\text{mes}}\mathscr{L}(\tilde{\chi})(s), \tag{1.88}$$
$$\mathcal{P}_\Omega(s) = \omega(s)P_\Omega(s)C_{\text{mes}}\mathscr{L}(\tilde{\chi})(s), \tag{1.89}$$
$$\mathcal{P}_w^0(s) = \omega(s)P_w^0(s)C_{\text{mes}}\mathscr{L}(\tilde{\chi})(s). \tag{1.90}$$

We have the following theorem:

Theorem 3 *Let $\omega(s)$ be any low pass filter with sufficiently high relative degree, and $0 < \tilde{\delta} < 1$ sufficiently small, such that*

$$\forall x \in \mathbb{R}, |1 - \omega(jx)| < \frac{1 - \tilde{\delta}}{||G_{obs}||_\infty \bar{\sigma}(P_{mes}(jx))}, \tag{1.91}$$

with
$$G_{obs}(s) = \int_0^{\frac{1}{\mu}} P_\upsilon(s,\mu\theta)e^{-s\theta}\mathrm{d}\theta + e^{-\frac{s}{\mu}}\left[\begin{bmatrix} C_{11} & C_{12}\end{bmatrix}(sI - A_1^{obs})^{-1}P_\Omega(s)\right.$$
$$\left. +\rho(e^{-\frac{s}{\lambda}}P_w^0(s) + \int_0^{\frac{1}{\lambda}} P_w(s,1-\lambda\theta)e^{-s\theta}\mathrm{d}\theta)\right]. \tag{1.92}$$

Consider the dynamic output feedback gains (1.87)-(1.90) *with $P_w(s,\theta)$, $P_\upsilon(s,\theta)$, $P_\Omega(s), P_w^0(s)$ defined by* (1.83)-(1.86)*. Then, under Assumptions 5 and 6, the*

[2] Due to the use of an adequate low-pass filter, this will however not prevent the output feedback control law to be robust with regard to small delays.

error system (1.73)-(1.78) *with any initial conditions in* $\mathcal{X}$ *is exponentially stable in the sense of the* $\mathcal{X}-$*norm.*

Proof The proof is omitted here due to space restrictions.

Thanks to Assumption 6, we are thus able to design dynamically observer gains stabilizing the target error system. Let us now define the original observer state

$$(\hat{X},\hat{u},\hat{v},\hat{Y}) = \mathcal{L}_{\text{obs}}^{-1}(\hat{\chi},\hat{w},\hat{\upsilon},\hat{\Omega}), \tag{1.93}$$

with $\mathcal{L}_{\text{obs}}^{-1}$ defined by (1.49)-(1.52). We have the following corollary

Corollary 1 *Let* $\omega(s)$ *be any low pass filter with sufficiently high relative degree, satisfying* (1.91) *and the dynamic output feedback of form* (1.87)-(1.90) *with* $P_w(s,\theta), P_\upsilon(s,\theta), P_\Omega(s), P_w^0(s)$ *defined by* (1.83)-(1.86)*. Then, under assumptions 5, 6, the observer state* (1.93) *converges towards the original state* (X,u,v,Y) *at an exponential rate.*

Proof Under the corollary assumptions, the target error state converges to zero at an exponential rate by Theorem 4. Consequently, the target observer state converges towards the target state. We therefore have access to an estimation of the state (χ,w,υ,Ω) with the observer state. Using the invertible backstepping transform $\mathcal{L}_{\text{obs}}^{-1}$ defined by (1.49)-(1.52), we then obtain an observer of the original state (X,u,v,Y). Indeed, we can define the original error state as $(\tilde{X},\tilde{u},\tilde{v},\tilde{Y}) = (X,u,v,Y) - (\hat{X},\hat{u},\hat{v},\hat{Y})$. Since the backstepping transform is invertible, the original error system shares same stability properties with the target error system, and is thus exponentially stable. Since the original error state converges to zero, the original observer is a correct estimation of the original state.

1.4.2 Output-feedback controller

We can now state the main result of this chapter

Theorem 4 *Consider the system* (1.1)-(1.6) *with the observer* (1.93),(1.68) (1.72) *and the control law*

$$\begin{aligned} U(s) = \; & (\tilde{F}_{\xi}(s)C_0 + F_0)[\hat{X}(s) - \int_0^1 K^{12}(y)\hat{u}(s,y) + K^{13}(y)\hat{v}(s,y)\mathrm{d}y \\ & +[-K^{14}\hat{Y}_1(s)]\tilde{F}_{\eta}(s) - (\tilde{F}_{\xi}(t)C_0 + F_0)K^{15}]\hat{Y}_2(s), \end{aligned} \tag{1.94}$$

with $\tilde{F}_{\xi}(t)$ *defined by* (1.43) *and* $\tilde{F}_{\eta}(s)$ *defined by* (1.46)*. Then, with any arbitrary initial conditions* $(X_0,u_0,v_0,Y_0) \in \mathcal{X}$*, the virtual output* $\epsilon(t)$ *is practically stabilized, i.e.* $|C_{e1}Y_1 + C_{e2}Y_2| \longrightarrow 0$*, and the norm of the state is bounded.*

Proof Using Theorem 2, we just need to show that the dynamics of $C_0\xi$ are stabilized by the output feedback law (1.94) in the absence of disturbance. By Corollary 1, the error state $(\tilde{X},\tilde{u},\tilde{v},\tilde{Y})$ exponentially converges to zero. Due to the invertibility of the backstepping transform $\mathcal{L}$, the target error state $(\tilde{\xi},\tilde{\alpha},\tilde{\beta},\tilde{\eta}) = \mathcal{L}(\tilde{X},\tilde{u},\tilde{v},\tilde{Y})$ exponentially converges to zero. In the Laplace domain, (1.45) with the proposed control law rewrites

$$\begin{aligned} C_0\mathscr{L}(\xi)(s) = \; & C_0(sI-\bar{A}_0)^{-1}(1-w(s))G(s)C_0\mathscr{L}(\xi)(s) \\ & -B_0\tilde{F}_{\xi}(s)\mathscr{L}(\tilde{\xi})(s) - B_0\tilde{F}_{\eta}(s)\mathscr{L}(\tilde{\eta}_p)(s). \end{aligned} \tag{1.95}$$

Since the error terms converge to zero due to Theorem 3, we use the variations of constants [16] to conclude that $C_0\xi$ converges to zero in the absence of disturbance.

1.5 Numerical simulation

In this section, we illustrate the performances of the state feedback controller on a test case. Due to lack of time, the observer has not been tested in simulation. The proposed approach was implemented using Matlab and Simulink. The transport PDE systems' evolution was simulated using an explicit in time, first-order, upwind finite difference method with 101 spatial discretization points. The ODE states were simulated using a stiff solver based on the second order Rosenbrock method (`ode23s`). The transfer functions in the control law were transformed to a state-space representation for implementation (`tf2ss`). The evolution of the systems were computed on a 50s time scale, with a CFL number equal to 0.9.
For the same initial system, we consider the tracking of a sinusoide reference trajectory in presence of a constant perturbation.

1.5.1 Presentation of the system

Let us first introduce the system described in Section 1.2.1, with the following numerical values: $\lambda = 2$, $\mu = 0.7$, $\sigma^+ = 1$, $\sigma^- = 0.5$, $\rho = 0.5$, $q = 1.2$. The ODE dynamics are in dimension $n = 4, m = 3, c = 2$[3], and defined by the matrices

$$A_0 = \begin{bmatrix} 0 & 0.14 & 0 & 0.1 \\ 0 & 0 & 0.14 & 0 \\ 0.29 & -0.43 & 0.57 & 0.2 \\ 0 & 0 & 0 & -1.1 \end{bmatrix}, B_0 = \begin{bmatrix} 0 & 0 \\ 0 & -1 \\ 1 & -1 \\ 0 & 0 \end{bmatrix}, C_0 = \begin{bmatrix} 1 & 0 & 0 & -0.5 \end{bmatrix}, E_0 = \begin{bmatrix} 2 \\ -1 \\ 0.1 \\ 0 \end{bmatrix},$$

[3] In this section, note that since the first component of $X(t)$ is a flat output, a scalar control should be sufficient.

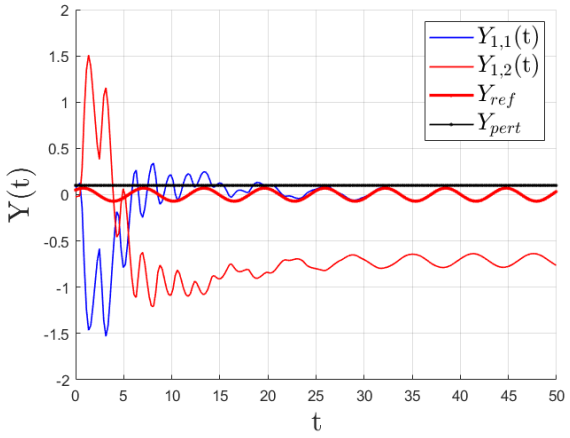

Fig. 1.4 Evolution of the state $Y(t)$

$$A_{11} = \begin{bmatrix} 0.29 & 0.14 & 0 \\ 0.14 & 0 & 0.1 \\ 0 & 0 & -0.9 \end{bmatrix}, E_1 = \begin{bmatrix} -1 \\ 1 \\ 0 \end{bmatrix}, C_{11} = \begin{bmatrix} 0 & 1 & 0.5 \end{bmatrix}.$$

With the numerical values chosen for the system, each ODE system and the PDE subsystem are independently unstable (and remain so when interconnected). Note that the system satisfies Assumption 1 since $\rho q = 0.6$. We can find matrices from Assumption 2 using pole placement. For the simulations, we used

$$F_0 = \begin{bmatrix} 41.71 & 5.43 & -1.93 & 0 \\ 42 & 5 & 0.14 & 0 \end{bmatrix}, F_1 = \begin{bmatrix} 12 & 8.71 & 0 \end{bmatrix}.$$

The kernels M^{ij}, K^{ij} are previously computed using a fixed-point algorithm (successive approximation technique). Their domains of definition are discretized using the same space mesh than (u, v)-state. The integral terms are numerically approximated by the trapezoidal method. Moreover, an input delay of 2.5ms was introduced in the control action to show the robustness of the design to small delays in the loop. The chosen w(s) is a simple 4th order low-pass filter with a bandwidth of approximately 100 rad/s.

1.5.2 Test case: trajectory tracking in presence of a disturbance

Let us consider a tracking problem, in which the second ODE state is subject to a constant disturbance $Y_{\text{pert}} = 0.1$. We want to follow a sinusoidal trajectory $Y_{\text{ref}}(t) = 0.1 \sin(t)$. We have an exogenous state with dynamics

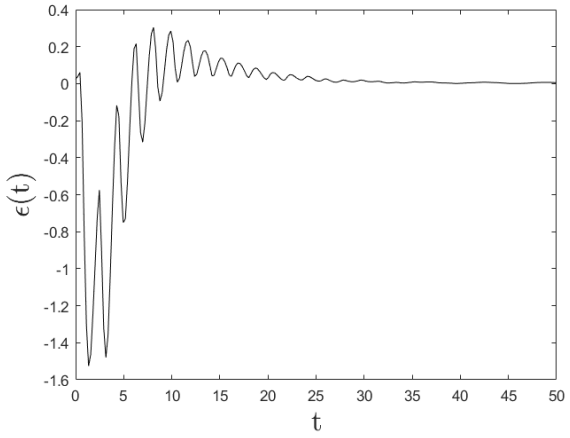

Fig. 1.5 Evolution of the virtual output $\epsilon(t)$

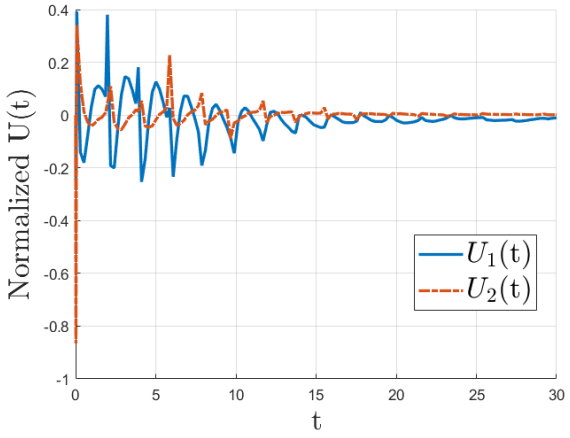

Fig. 1.6 Evolution of the normalized state-feedback effort $U(t)$

$$\dot{Y}_2(t) = A_{22}Y_2(t) = \begin{bmatrix} 0 & 0 & 0 \\ 0 & 0 & 1 \\ 0 & -1 & 0 \end{bmatrix} \begin{bmatrix} Y_{\text{pert}} \\ Y_{\text{ref}} \\ \dot{Y}_{\text{ref}} \end{bmatrix}.$$

As previously, the constant perturbation acts on the first component of $Y_1(t)$ and on the boundaries of the PDE system

$$A_{12} = \begin{bmatrix} 1 & 0 & 0 \\ 0 & 0 & 0 \\ 0 & 0 & 0 \end{bmatrix}, \quad C_{12} = \begin{bmatrix} 0.1 & 0 & 0 \end{bmatrix}.$$

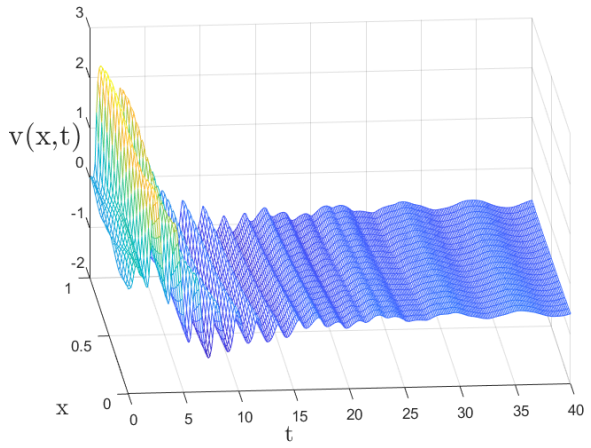

Fig. 1.7 Evolution of the leftward convecting PDE state $v(t,x)$

Notice that $A_{12} \notin Im(E_1)$ (unmatched disturbance), $E_1C_1 = 0$, $C_0B_0 = 0$, $E_0 \notin Im(B_0)$ and (A_0, B_0) is not controllable but is stabilizable. The numerical values were chosen such that the disturbance cannot be algebraically cancelled by the control law, which must take into account the dynamics of the system. The initial conditions are given by $u_0(x) = 0.05\sin(10x)$, $v_0(x) = 0.1\cos(13x)$ and $X(0) = \begin{bmatrix}-0.2 & -1 & -2 & -2\end{bmatrix}^T$, $Y(0) = 0.5 \times \begin{bmatrix}0.15 & -0.05 & 0.1 & 0.2 & 0.1 & 0.1\end{bmatrix}^T$. We have $C_e = \begin{bmatrix}1 & 0 & 0 & 0 & -1 & 0\end{bmatrix}$, such that the first component of the output follows the sinusoidal trajectory by stabilizing $\epsilon(t) = Y_{1,1}(t) - Y_{\text{ref}}(t)$. Note that the input ODE system and the PDE systems do not converge towards a constant value, but follow a sinusoidal dynamics as expected (Figure 1.7). The control effort is represented on Figure 1.6. Due to the high level of instability of the original system, the initial effort presents high values. The effect of saturation is out of the scope of this chapter, but should be investigated for further applications on real systems. The control effort remains continuous for any L^2 initial conditions.

1.6 Notes, comments and concluding remarks

In this chapter, a strictly proper dynamic output-feedback controller was designed for the practical output regulation and output tracking of a class of 2×2 linear hyperbolic ODE-PDE-ODE systems. The load dynamics (the unactuated end of the PDE) were dynamically augmented with a finite-dimensional exosystem modeling possible trajectory and disturbance inputs. The proposed approach was based on a backstepping transform that allowed us to reformulate the regulation problem in terms of a time-delay system with

pointwise and distributed delays. We also followed the backstepping methodology to design an observer for the state and disturbance reconstruction. We used frequency analysis to design a feedback controller robust to small delays by extending the filtering techniques used in [8].
The omitted proofs and more computational details can be found in [21]. In future works, we will focus on implementation aspects (saturation of the effort, numerical observer design) to apply the proposed methodology to industrial applications. The performances of the feedback controller will be compared to PI controllers.

References

1. Aamo, O.M, Disturbance rejection in 2×2 linear hyperbolic systems. IEEE Transactions on Automatic Control, 58(5), 1095-1106, 2013.
2. Aarsnes, U. J. and Di Meglio, F. and Shor, R.J. Avoiding stick slip vibrations in drilling through startup trajectory design. Journal of Process Control, 70, 24–35, 2018.
3. Aarsnes, U.J.F and Di Meglio, F. and Evje,S. and Aamo, O.-M. Control-oriented drift-flux modeling of single and two-phase flow for drilling. ASME 2014 Dynamic Systems and Control Conference, 2014.
4. Auriol, J. and Aarsnes, U. J. F. and Martin, P. and Di Meglio, F. Delay-robust control design for heterodirectional linear coupled hyperbolic PDEs. IEEE Transactions on Automatic Control, 2018.
5. Auriol, J. and Kazemi, N. and Innanen, K. and Shor, R. Combining formation seismic velocities while drilling and a PDE-ODE observer to improve the drillstring dynamics estimation. IEEE American Control Conference (ACC), 2020.
6. Bastin, G. and Coron, J.-M. Stability and boundary stabilization of 1-D hyperbolic systems. Springer, 2016.
7. Bou Saba, D. and Bribiesca-Argomedo, F. and Di Loreto, M. and Eberard, D. Backstepping stabilization of 2×2 linear hyperbolic PDEs coupled with potentially unstable actuator and load dynamics. IEEE 56th Annual Conference on Decision and Control (CDC), 2498-2503, 2017.
8. Bou Saba, D. and Bribiesca-Argomedo, F. and Di Loreto, M. and Eberard, D. Strictly Proper Control Design for the Stabilization of 2×2 Linear Hyperbolic ODE-PDE-ODE Systems. IEEE 58th Conference on Decision and Control (CDC), 2019.
9. Deutscher, J. and Gehring, N. and Kern, R. Output feedback control of general linear heterodirectional hyperbolic ODE–PDE–ODE systems. Elsevier Automatica, 95, 472–480, 2018.
10. Deutscher, J. and Gehring, N. and Kern, R.: Output feedback control of general linear heterodirectional hyperbolic ODE-PDE-ODE systems. Automatica, 2018, vol. 95, pp. 472-480.
11. Deutscher, J. and Gabriel, J. A backstepping approach to output regulation for coupled linear wave–ODE systems. Elsevier Automatica, 123, 109338, 2021.
12. Di Meglio, F. and Bribiesca Argomedo, F. and Hu, L. and Krstic, M. Stabilization of coupled linear heterodirectional hyperbolic PDE–ODE systems. Elsevier Automatica, 87, 281–289, 2018.
13. Di Meglio, F. and Lamare, P.-O. and Aarsnes, U. J. F. Robust output feedback stabilization of an ODE–PDE–ODE interconnection. Elsevier Automatica, 119, 109059, 2020.

14. Francis, B. A. and Wonham, W. M. The internal model principle for linear multivariable regulators. Applied mathematics and optimization, 2(2), 170–194, 1975.
15. Guerrero, M. E. and Mercado, D. A. and Lozano, R. and García, C. D. Passivity based control for a quadrotor UAV transporting a cable-suspended payload with minimum swing. 54th IEEE Conference on Decision and Control (CDC), 6718-6723, 2015.
16. Hale, J.K. and Verduyn Lunel, S.M.: Introduction to functional differential equations. Springer-Verlag, 1993
17. Kern, R. and Gehring, N. and Deutscher, J. and Meissner, M. Design and Experimental Validation of an Output Feedback Controller for a Pneumatic System with Distributed Parameters. S18th International Conference on Control, Automation and Systems (ICCAS), 1391–1396, 2018.
18. Krstic, M. and Smyshlyaev, A. Backstepping boundary control for first-order hyperbolic PDEs and application to systems with actuator and sensor delays. Systems & Control Letters, 57(9), 750–758, 2008.
19. Krstic, M. and Smyshlyaev, A. Boundary control of PDEs: A course on backstepping designs. SIAM, 16, 2008.
20. Logemann, H. and Rebarber, R. and Weiss, G. Conditions for robustness and nonrobustness of the stability of feedback systems with respect to small delays in the feedback loop. SIAM Journal on Control and Optimization, 34(2), 572–600, 1996.
21. Redaud, J. and Bribiesca Argomedo, F. and Auriol, J. Output Regulation and Tracking for Linear ODE-Hyperbolic PDE-ODE systems. Elsevier Automatica (to be submitted), 2022.
22. Schmuck, C. and Woittennek, F. and Gensior, A. and Rudolph, J. Flatness-based feed-forward control of an HVDC power transmission network. IEEE 33rd International Telecommunications Energy Conference (INTELEC), 1–6, 2011.
23. Smith, O. A controller to overcome dead time. ISA J., 6, 28–33, 1959.
24. Vazquez, R. and Krstic, M. and Coron, J.-M. Backstepping boundary stabilization and state estimation of a 2×2 linear hyperbolic system. 50th IEEE Conference on Decision and Control (CDC), 4937–4942, 2011.
25. Wang, J. and Krstic, M. Delay-compensated control of sandwiched ODE-PDE-ODE hyperbolic systems for oil drilling and disaster relief. Elsevier Automatica, 120,109131, 2020.
26. Yoshida, K. Lectures on differential and integral equations. Interscience Publishers, 10, 1960.